Transverse Electromagnetic Modes in Aperture Waveguides Containing a Metamaterial with Extreme Anisotropy

Peter B. Catrysse* and Shanhui Fan†

E. L. Ginzton Laboratory and Department of Electrical Engineering, Stanford University, California 94305, USA

(Received 21 November 2010; revised manuscript received 12 April 2011; published 2 June 2011)

We use metamaterials with extreme anisotropy to solve the fundamental problem of light transport in deep subwavelength apertures. By filling a simply connected aperture with an anisotropic medium, we decouple the cutoff frequency and the group velocity of modes inside apertures. In the limit of extreme anisotropy, all modes become purely transverse electromagnetic modes, free from geometrical dispersion, propagate with a velocity controlled by the transverse permittivity and permeability, and have zero cutoff frequency. We analyze physically realizable cases for a circular aperture and show a metamaterial design using existing materials.

DOI: 10.1103/PhysRevLett.106.223902 PACS numbers: 42.82.Et, 42.25.Bs, 78.20.Ci, 78.67.Pt

Metamaterials with extreme properties have generated significant basic physics interest in recent years. Notable examples include epsilon-near-zero materials [1,2], ultralow refractive-index materials [3], and ultrahigh refractive-index materials [4–6]. Many photonic structures, such as waveguides, lenses, and photonic band gap materials, benefit greatly from the very large index contrast provided by these metamaterials [7,8]. Metamaterials with extreme anisotropy offer another level of flexibility. This has already led to novel behaviors and control over material properties, such as nonmagnetic left-handedness and photonic density-of-states engineering [9–12].

In this work, we point out that metamaterials with extreme anisotropy can be used to solve a fundamental problem that is of both great importance and practical interest in nanophotonics: efficient light transport in deep subwavelength apertures. We define a subwavelength aperture here as simply connected and with both transverse dimensions at the subwavelength scale. An example of such an aperture would be a hole made in a metal or polar material film with a cross section that is significantly smaller than the operating wavelength [13–15]. While traditional deep subwavelength apertures do not support guided modes, our approach turns these apertures into waveguides. Such an aperture waveguide enables efficient light transport, which is of fundamental importance for light manipulation light at deep subwavelength length scales and of practical significance for many photonic devices and applications [16,17].

In general, the optical behavior of a single aperture is determined by the dispersion relation of the corresponding waveguide structure with the same cross-sectional geometry as the aperture [13]. Subwavelength apertures typically transmit light with an efficiency that is substantially below unity, because the corresponding waveguide exhibits evanescent decay of electromagnetic fields below the cutoff frequency [16]. One simple approach for lowering the cutoff frequency and potentially allowing efficient light transport in deep subwavelength holes is to fill them with a high-index dielectric medium. If the medium is isotropic, however, both the cutoff frequency and the group velocity are lowered simultaneously. In particular, the maximum group velocity is reduced, leading to slow light operation. Such a trade-off is not always desirable: Reducing group velocity can adversely impact signal transport and often increases the impact of loss thereby lowering light throughput.

Here, we demonstrate that, by filling the hole with an anisotropic medium, it is possible to decouple the cutoff frequency and the maximum group velocity. We consider a uniaxial anisotropic medium described by its permittivity and permeability tensors

$$\bar{\bar{\varepsilon}} = \varepsilon_0 \begin{pmatrix} \varepsilon_\perp & 0 & 0 \\ 0 & \varepsilon_\perp & 0 \\ 0 & 0 & \varepsilon_z \end{pmatrix}, \quad \bar{\bar{\mu}} = \mu_0 \begin{pmatrix} \mu_\perp & 0 & 0 \\ 0 & \mu_\perp & 0 \\ 0 & 0 & \mu_z \end{pmatrix}. \tag{1}$$

ε_0 and μ_0 represent the vacuum permittivity and permeability, respectively, while $\varepsilon_\perp$ ($\mu_\perp$) and ε_z (μ_z) are the relative transverse and longitudinal permittivity (permeability), respectively. In the limit of extreme anisotropy ($\varepsilon_z \to \infty$, $\mu_z \to \infty$), we show that all modes in a hole become purely transverse electromagnetic (TEM) modes and that they all have a zero cutoff frequency, while retaining a substantial group velocity. This is a rather novel effect. In conventional simply connected apertures, by contrast, modes possess a nonzero longitudinal electric or magnetic field component and have a finite cutoff frequency.

A hole with perfect electric conducting (PEC) sidewalls, in general, supports either purely transverse electric (TE) modes ($E_z = 0, H_z \neq 0$) or transverse magnetic (TM) modes ($H_z = 0$, $E_z \neq 0$). When the hole is filled with a dielectric medium that exhibits extreme anisotropy ($\varepsilon_z \rightarrow \infty$, $\mu_z \rightarrow \infty$), however, all modes become purely TEM modes ($E_z = 0$, $H_z = 0$). To demonstrate this, the anisotropic medium [Eq. (1)] is placed at the core of a cylindrical waveguide (hole) with its axis along the z direction. Assuming the field components are $\propto \exp(-i\omega t)$ with frequency ω, we find for the z component of the curl equations

$$(\nabla \times \mathbf{H})_z = -i\omega\varepsilon_0\varepsilon_z E_z, \quad (\nabla \times \mathbf{E})_z = i\omega\mu_0\mu_z H_z. \tag{2}$$

The left-hand sides of Eq. (2) are finite. Hence, the longitudinal components E_z and H_z must vanish ($E_z = 0$ and $H_z = 0$) in the limit of extreme anisotropy $\varepsilon_z \rightarrow \infty$, $\mu_z \rightarrow \infty$. All modes therefore become purely TEM modes. This result is valid for holes with an arbitrary cross section. For holes with sidewalls made of any material, our result remains valid for the field profile inside the hole.

We now show that the dispersion relation of these modes is free from geometrical dispersion and without cutoff. For this proof, we start again by considering a general waveguide (aperture) filled with a dielectric medium described by Eq. (1). We treat TM and TE modes separately in the appropriate limit of ε_z, $\mu_z \rightarrow \infty$. For TM modes, the nonzero field components are the transverse electric, magnetic vector fields $\mathbf{E}_\perp$ and $\mathbf{H}_\perp$ and the longitudinal electric field component E_z; they satisfy the following equations:

$$\nabla_\perp \times \mathbf{H}_\perp + \frac{\partial}{\partial z}\mathbf{e_z} \times \mathbf{H}_\perp = -i\omega\varepsilon_0(\varepsilon_\perp \mathbf{E}_\perp + \varepsilon_z E_z \mathbf{e_z}), \tag{3}$$

$$\nabla_\perp \times \mathbf{E}_\perp + \frac{\partial}{\partial z}\mathbf{e_z} \times \mathbf{E}_\perp = i\omega\mu_0\mu_\perp \mathbf{H}_\perp, \tag{4}$$

where $\mathbf{e_z}$ is the unit vector in the z direction. In Eq. (4), we used that $E_z = 0$ when $\varepsilon_z \rightarrow \infty$. We assume that all field components are $\propto \exp(i\beta z)$, where β is the wave vector. Equations (3) and (4) can both be split into their transverse and longitudinal parts:

$$\begin{aligned} \nabla_\perp \times \mathbf{H}_\perp &= -i\omega\varepsilon_0\varepsilon_z E_z \mathbf{e_z}, \\ \beta\mathbf{e_z} \times \mathbf{H}_\perp &= -\omega\varepsilon_0\varepsilon_\perp \mathbf{E}_\perp, \end{aligned} \tag{5}$$

$$\nabla_\perp \times \mathbf{E}_\perp = 0, \qquad \beta\mathbf{e_z} \times \mathbf{E}_\perp = \omega\mu_0\mu_\perp \mathbf{H}_\perp. \tag{6}$$

We then combine the expressions for the transverse fields in Eqs. (5) and (6) and arrive at the dispersion relation of the TM modes,

$$\omega = v_{\mathrm{aniso}}\beta, \tag{7}$$

where $v_{\mathrm{aniso}} = c/\sqrt{\varepsilon_\perp\mu_\perp}$. A treatment for TE modes yields an expression identical to Eq. (7).

The analysis above shows that in an aperture filled with an extreme anisotropic medium ($\varepsilon_z \rightarrow \infty$, $\mu_z \rightarrow \infty$) all modes are free from geometrical dispersion with a velocity v_{aniso} (group velocity = phase velocity) that is entirely controlled by the transverse permittivity and permeability and have zero cutoff frequency. Moreover, all modes are degenerate with the dispersion relation of a TEM mode [Eq. (7)]. These properties are quite unusual for an aperture with a simply connected cross section.

For an in-depth analysis of physically realizable cases, i.e., for ε_z, μ_z finite but very large compared to $\varepsilon_\perp$, $\mu_\perp$, we now consider a hole with a circular cross section of radius r_0. All modes in this system can be calculated analytically. We employ an exact one-dimensional finite-difference frequency-domain method in cylindrical coordinates (r, θ, z) to visualize them [18]. For illustration, we focus on the lowest-order TE and TM modes (TE_{11}, TM_{01}, TE_{21}, and TM_{11}). In calculating the dispersion curves (β, ω), we assume a uniaxial anisotropic dielectric with $\varepsilon_\perp = 2.13$, $\varepsilon_z = 2130$, $\mu = 1$ and $\varepsilon = 2.13$, $\mu_\perp = 1$, $\mu_z = 1000$. We also calculate the dispersion curves for an isotropic dielectric with $\varepsilon = 2.13$ and $\mu = 1$, as well as for one with $\varepsilon = 2130$ and $\mu = 1000$.

For a waveguide filled with an isotropic dielectric medium, the dispersion relations for the TM and TE modes are well-known [19]:

$$\omega^2 = v^2\beta^2 + \omega^2_{c,\mathrm{TM}_{mn}}, \qquad \omega^2 = v^2\beta^2 + \omega^2_{c,\mathrm{TE}_{mn}}, \tag{8}$$

with $v = c/\sqrt{\varepsilon\mu}$ and cutoff frequencies $\omega_{c,\mathrm{TM}_{mn}} = h_{\mathrm{TM}}c/\sqrt{\mu\varepsilon}$ and $\omega_{c,\mathrm{TE}_{mn}} = h_{\mathrm{TE}}c/\sqrt{\varepsilon\mu}$. The constants h_{TM} and h_{TE} depend on the mode order (m, n), according to boundary conditions for E_z and H_z at $r = r_0$ [19]. As shown in Fig. 1(a) ($\varepsilon = 2.13$ and $\mu = 1$), the dispersion curves go to nonzero cutoff frequencies when $\beta \rightarrow 0$.

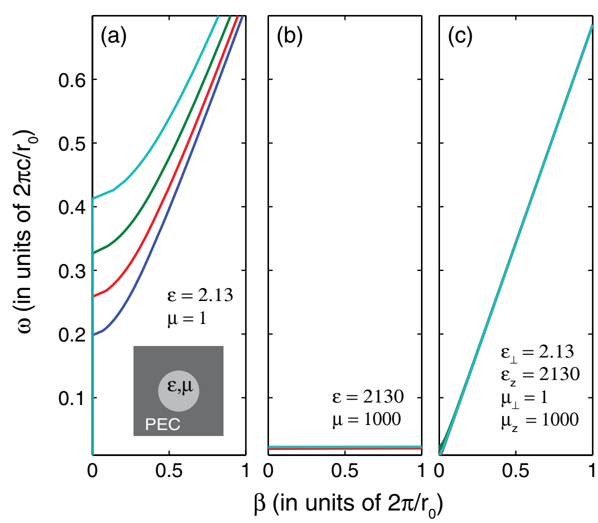

FIG. 1 (color online). Dispersion diagram (β, ω) for the lowest-order modes supported by a circular waveguide with PEC walls and filled with (a),(b) an isotropic dielectric ($\varepsilon = 2.13$ and $\mu = 1$, $\varepsilon = 2130$ and $\mu = 1000$) and (c) a uniaxial anisotropic dielectric ($\varepsilon_\perp = 2.13$, $\varepsilon_z = 2130$, $\mu = 1$ for TM modes, and $\varepsilon = 2.13$, $\mu_\perp = 1$, $\mu_z = 1000$ for TE modes). The solid blue, red, green, and cyan curves are for the TE_{11}, TM_{01}, TE_{21}, and TM_{11} modes, respectively (in order of ascending cutoff).

For large β, all curves approach the light line of the isotropic dielectric $\omega = v\beta$. Figure 1(b) illustrates the simple approach towards lowering cutoff frequency, i.e., filling the hole with an isotropic medium with large permittivity and permeability ($\varepsilon = 2130$ and $\mu = 1000$). In addition to lowering the cutoff frequency, this approach also dramatically reduces group velocity (flat dispersion curves). By contrast, Fig. 1(c) describes the dispersion curves in the case of extreme anisotropy ($\varepsilon_\perp = 2.13$, $\varepsilon_z = 2130$, $\mu = 1$ for TM modes and $\varepsilon = 2.13$, $\mu_\perp = 1$, $\mu_z = 1000$ for TE modes). All TM (TE) modes exhibit extremely low (near-zero) cutoff frequencies but also retain substantial maximum group velocities.

Figure 2 shows the transverse electric field distributions for the lowest-order modes in the anisotropic waveguide (hole). They are obtained by using the finite-difference frequency-domain method. The modes have distinct transverse distributions that closely resemble those of the TM (TE) modes in an isotropic waveguide [19]. This is expected. In both the anisotropic *and* the isotropic case, the transverse fields for the TM (TE) modes satisfy $\nabla_\perp^2 \mathbf{H}_\perp + h_{\mathrm{TM}}^2 \mathbf{H}_\perp = 0$ ($\nabla_\perp^2 \mathbf{E}_\perp + h_{\mathrm{TE}}^2 \mathbf{E}_\perp = 0$) and $\mathbf{D}_\perp = -\beta(\mathbf{e}_z \times \mathbf{H}_\perp)/\omega$ [$\mathbf{B}_\perp = \beta(\mathbf{e}_z \times \mathbf{E}_\perp)/\omega$]. These equations are identical in both cases with the constant h_{TM} (h_{TE}) determined by cross-sectional geometry (boundary conditions) and mode order only. Hence, the field profiles should be identical as well for modes with the same h_{TM} (h_{TE}) independent of (an)isotropy. In the extreme anisotropic case ($\varepsilon_\perp = 2.13$, $\varepsilon_z = 2130$, $\mu = 1$ for TM modes and $\varepsilon = 2.13$, $\mu_\perp = 1$, $\mu_z = 1000$ for TE modes), however, the modes feature these distinct transverse field profiles while having near-zero longitudinal fields $H_z = 0$ and $E_z \simeq 0$ for TM ($E_z = 0$ and $H_z \simeq 0$ for TE).

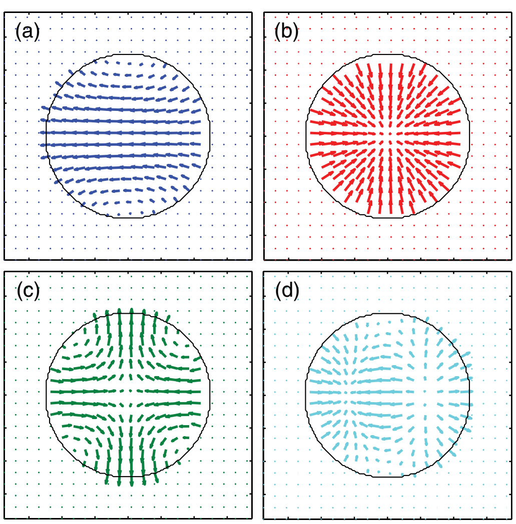

FIG. 2 (color online). Transverse electric vector field $\mathbf{E}_\perp$ for the lowest-order modes of a circular waveguide with PEC cladding and filled with a uniaxial anisotropic dielectric with (b),(d) $\varepsilon_\perp = 2.13$, $\varepsilon_z = 2130$, $\mu = 1$ for TM modes and (a), (c) $\varepsilon = 2.13$, $\mu_\perp = 1$, $\mu_z = 1000$ for TE modes.

Figure 3 shows the cutoff frequency for the lowest-order TM modes ($\omega_c = \omega_{c,\mathrm{TM}_{mn}}$) as a function of the ratio between the longitudinal (ε_z) and the transverse ($\varepsilon_\perp$) permittivity when $\varepsilon_\perp = 2.13$, as well as for lowest-order TE modes ($\omega_c = \omega_{c,\mathrm{TE}_{mn}}$) as a function of the ratio between the longitudinal (μ_z) and the transverse ($\mu_\perp$) permeability when $\mu_\perp = 1$. As the ratio increases ($\varepsilon_z \to \infty$ or $\mu_z \to \infty$), the cutoff frequency goes to zero. We also graph the maximum group velocity for each mode and observe that the velocity does not vary with the permittivity (permeability) ratio. It remains at the value of the velocity in an isotropic medium with $\varepsilon = 2.13$ and $\mu = 1$. This shows the absence of a trade-off; i.e., the cutoff frequency can be lowered arbitrarily without affecting the maximum group velocity. The analytic prediction that we made with $\varepsilon_z \to \infty$ and $\mu_z \to \infty$ can therefore be realized in physical systems by making ε_z, μ_z much larger compared to $\varepsilon_\perp$, $\mu_\perp$.

The combination of simultaneous small (finite) transverse permittivity or permeability and large (infinite) longitudinal permittivity or permeability is typically hard to find in naturally occurring materials. Metamaterial design, however, offers an approach for designing a medium with such an extreme anisotropy. The required anisotropy can be obtained by alternating concentric layers of dielectric media with low and high relative permittivity. When the thickness of each individual layer is much less than the operating wavelength, we can treat this finely structured material as an effective dielectric with

$$\varepsilon_r = \frac{\varepsilon_1 \varepsilon_2}{(1-f)\varepsilon_1 + f\varepsilon_2}, \qquad \varepsilon_z = f\varepsilon_1 + (1-f)\varepsilon_2, \quad (9)$$

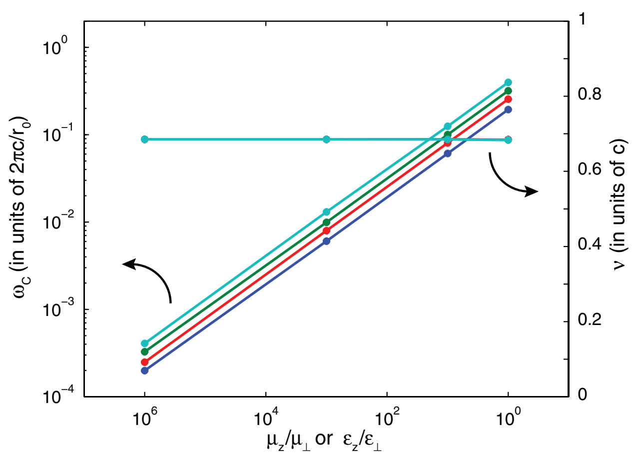

FIG. 3 (color online). Cutoff frequency and maximum group velocity for a circular waveguide with PEC cladding and filled with a uniaxial anisotropic dielectric. Cutoff frequency ω_c and maximum group velocity v are graphed as a function of $\mu_z/\mu_\perp$ for the TE_{11} (blue curve) and TE_{21} (green curve) modes and as a function of $\varepsilon_z/\varepsilon_\perp$ for the TM_{01} (red curve) and TM_{11} (cyan curve) modes.

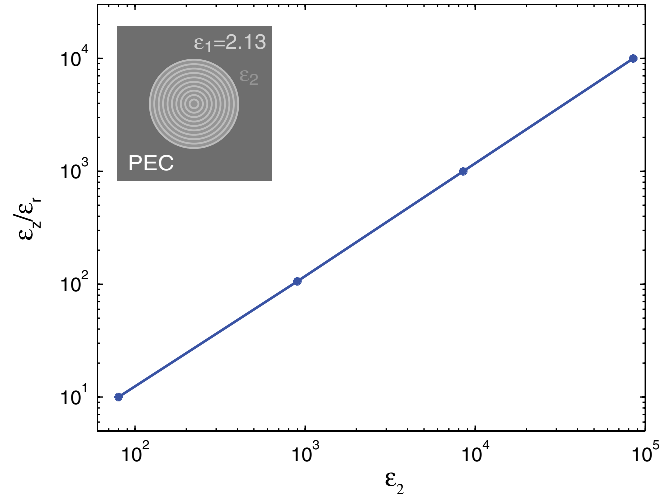

FIG. 4 (color online). Metamaterial design for a dielectric with extreme anisotropy based on alternating concentric rings of a high (ε_2) and a low (ε_1) permittivity dielectric medium. $\varepsilon_z/\varepsilon_r$ for the uniaxial anisotropic metamaterial is graphed versus ε_2 (for $\varepsilon_1 = 2.13$). The inset shows the cross section of the aperture and metamaterial geometry.

where ε_1 and ε_2 are the relative permittivities of the component media, while f and $1 - f$ are the fractions of the total volume occupied by each of the respective media [20]. We note that the field distribution of $\mathbf{E}_\perp$ for the lowest-order TM_{01} mode is purely radial and thus $\varepsilon_\perp = \varepsilon_r$. The ratio of ε_z to ε_r is maximized when $f = 1/2$, thereby simultaneously achieving a low cutoff frequency while maintaining significant maximum group velocity. Figure 4 shows the ratio $\varepsilon_z/\varepsilon_r$ as a function of ε_2 (for $\varepsilon_1 = 2.13$). In particular, $\varepsilon_z/\varepsilon_r$ reaches $\sim$10 000 if we use a dielectric with $\varepsilon_2 = 85\,000$. Dielectrics with such large relative permittivities exist up to radio frequencies [21].

As another example, we create a metamaterial in the microwave regime that combines $Ba_{0.6}Sr_{0.4}TiO_3$, which has a permittivity of 900 at 2 GHz [22], and Teflon ($\varepsilon = 2.1$). We find that the cutoff frequency of the TM_{01} mode, in a 3-mm radius hole filled with such a metamaterial, is reduced by more than an order of magnitude from $\omega_{c,\mathrm{TM}_{01}} = 26.4$ GHz (for a hole filled with Teflon $\varepsilon = 2.1$) to $\omega^{\mathrm{aniso}}_{c,\mathrm{TM}_{01}} = 1.8$ GHz (for a hole filled with the uniaxial anisotropic metamaterial with $\varepsilon_r = 4.2$ and $\varepsilon_z = 451.1$), while the maximum group velocity changes by less than a factor of 2 (compared to a group velocity that is more than 20 times smaller in $Ba_{0.6}Sr_{0.4}TiO_3$). It is important to note, in this context, that the extremely large values for ε_2 are required only near the cutoff frequency. In particular, to achieve this behavior over a wide range of frequencies, large permittivity values are needed only at the low end of the frequency range. In general, materials with larger permittivity are found at lower frequencies. Thus the approach proposed here can be useful in designing apertures with extremely broad bandwidth. For the fabrication of such structures, finally, there exist self-assembly approaches for creating cylindrical periodic structures with nanosize periods [23], as well as conformal coating methods for achieving thin nanolayers of polymers around nanowires [24].

This research is supported in part by the Department of Energy, Grant No. DE-FG02-07ER46426.

*pcatryss@stanford.edu
†shanhui@stanford.edu

[1] M. Silveirinha and N. Engheta, Phys. Rev. Lett. **97**, 157403 (2006).
[2] B. Edwards *et al.*, Phys. Rev. Lett. **100**, 033903 (2008).
[3] B. T. Schwartz and R. Piestun, J. Opt. Soc. Am. B **20**, 2448 (2003).
[4] J. T. Shen, P. B. Catrysse, and S. H. Fan, Phys. Rev. Lett. **94**, 197401 (2005).
[5] J. Shin *et al.*, IEEE J. Sel. Top. Quantum Electron. **12**, 1116 (2006).
[6] J. Shin, J. T. Shen, and S. H. Fan, Phys. Rev. Lett. **102**, 093903 (2009).
[7] B. T. Schwartz and R. Piestun, Appl. Phys. Lett. **85**, 1 (2004).
[8] J. Christensen and F. J. Garcia de Abajo, Phys. Rev. B **82**, 161103(R) (2010).
[9] V. A. Podolskiy and E. E. Narimanov, Phys. Rev. B **71**, 201101 (2005).
[10] J. Yao *et al.*, Science **321**, 930 (2008).
[11] A. J. Hoffman *et al.*, Nature Mater. **6**, 946 (2007).
[12] Z. Jacob *et al.*, Appl. Phys. B **100**, 215 (2010).
[13] P. B. Catrysse and S. H. Fan, J. Nanophoton. **2**, 021790 (2008).
[14] K. J. Webb and J. Li, Phys. Rev. B **73**, 033401 (2006).
[15] P. B. Catrysse and S. H. Fan, Phys. Rev. B **75**, 075422 (2007).
[16] F. J. Garcia-Vidal *et al.*, Rev. Mod. Phys. **82**, 729 (2010).
[17] T. W. Ebbesen *et al.*, Nature (London) **391**, 667 (1998).
[18] P. B. Catrysse and S. H. Fan, Appl. Phys. Lett. **94**, 231111 (2009).
[19] U. S. Inan and A. S. Inan, *Electromagnetic Waves* (Prentice-Hall, Upper Saddle River, NJ, 2000), pp. 354–364.
[20] M. Born and E. Wolf, *Principles of Optics* (Pergamon, New York, 1980).
[21] C. Pecharroman *et al.*, Adv. Mater. **13**, 1541 (2001).
[22] L. Wu *et al.*, Jpn. J. Appl. Phys. **38**, 5612 (1999).
[23] Q. Li *et al.*, Phys. Rev. Lett. **92**, 186102 (2004).
[24] S. R. Gowda *et al.*, Nano Lett. **11**, 101 (2011).